21th International Conference on Renewable Energies and Power Quality (ICREPQ'23)
Madrid (Spain), 24th to 26th May 2023
Renewable Energy and Power Quality Journal (RE&PQJ)
ISSN 2172-038 X, Volume No.21, July 2023

An Enhanced Hybrid Grid Connected Photovoltaic System Using Voltage Oriented Controller and Class D Chopper

Maamar Taleb [1], Mohamed Amine Fnaiech [1] and Khaled Zehar[1]

[1] Department of Electrical and Electronics Engineering,
College of Engineering, University of Bahrain,
P.O.Box 32038, Isa Town, Bahrain
Phone:+0097339151520, e-mail: **mtaleb@uob.edu.bh, mfnaiech@uob.edu.bh, kzehar@uob.edu.bh**

Abstract. The performance of a shunt interconnection made from a PV system, a three phase grid voltage supply, and a DC shunt motor (DC load) is investigated The PV system participates with maximum powers to the overall interconnection active power flow. It uses a class D chopper circuitry controlled properly by a typical maximum power point tracker (MPPT) controller. The grid has the role of supplying active power in case of any power deficiency needed by the DC motor load. Similarly, it has also the role of absorbing active power in case of any additional power generated by the PV system and not needed by the DC load. This is done by using an AC/DC power electronic converter. The AC/DC power electronic converter operates either under rectifier or inverter modes. The AC/DC power electronic converter is also operated under the next two conditions: 1-the reactive power expected at the grid voltage bus should be nearly null, 2-harmonics currents often encountered in the grid line currents waveforms should be tolerable. The two latter conditions are fulfilled by using the principle of voltage oriented control (VOC) technique. The performance of the investigated interconnection is simulated in Matlab/Simulink platform. Quite satisfactory results are obtained. The satisfaction about the obtained simulation results persists on being able to integrate easily the PV system with the AC grid while extracting maximum power from the PVG and having a unity power factor at the AC grid bus and less encountered harmonics in the ac line currents.

Key words. Grid-Tied Photovoltaic (PV) system; AC/DC Converter; Class D Chopper; Maximum Power Point Tracker; Perturb and Observe Control Technique; Voltage Oriented Control.

1. Introduction

Due to the ongoing cost reduction of photovoltaic modules, the power production by solar photovoltaic systems is growing fast. Experts anticipate that solar photovoltaic systems will have an enormous impact in global electric energy production in the future. This is quite true in countries that are blessed by quite good yearly solar irradiations levels like the ones in the Middle East and North Africa regions.

Two decades ago, most of the solar photovoltaic systems were standalone electricity generating systems. But, with the increased energy demand, large-scale photovoltaic grid-connected technology has gained more implementation worldwide [1]. The advantage of the photovoltaic grid connected systems is that they are connected easily with the grid circuitry through power electronic AC/DC converters and do not need storage batteries. Cancelling the storage batteries from the integrated hybrid grid-PV setups decreases the overall capital cost of the resulted renewable energy installations.

Figure 1 represents a basic sketch of a conventional grid-connected photovoltaic system. The photovoltaic system (PV) is linked to the grid through a power electronic inverter.

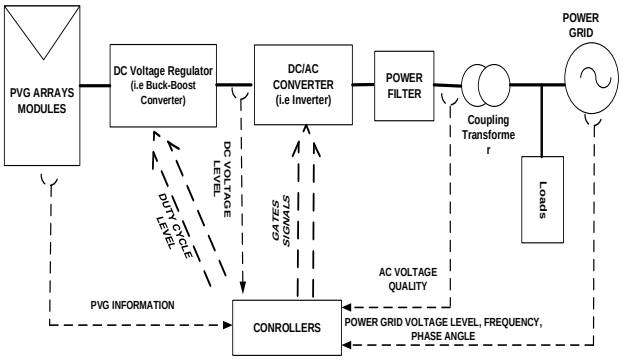

Fig1. A Typical Grid-Tied PV System

Actually, the inverter harvests the power from the photovoltaic energy arrays and changes its form from a DC power to AC power. The inverter should make sure that resulted AC power is in conformity with the grid regulations limits.

When operating a grid-connected photovoltaic through an inverter, as an interface and when the latter is controlled by the different Pulse Width Modulation (PWM) techniques, many problems or inconveniences are noted. The problems may include voltage stability, frequency variation, and distortion in current and voltages time varying waveforms. References [2-3] enumerate some side effects of grid-connected photovoltaic power plants on the performance of power grid constituents.

To maximize electric power generation from photovoltaic systems, a number of research works has been established to address certain raised concerns. The research works concentrated on either improving the performance of photovoltaic panels or controlling adequately the power electronic interface circuitry. In the

field of controlling the power electronics circuitry, two points are mainly considered: In the first point, several papers discussed the development of Maximum Power Point Tracking (MPPT) algorithms to maximize the output power from the photovoltaic systems [4-5]. In the second point, the use of inverters controlled by pulse width modulation techniques and the need for filters to improve the quality of the power injected into the grid are discussed [6-7]. In reference [8], both above aspects have been considered where a grid-connected PV system is proposed. It used the MPPT technique to calculate the phase angle between the inverter voltage and the grid voltage to determine the optimal slope of the power load line. This corresponded to the maximum power point of the PVG generator.

In the main author's previous works [9], PV arrays were connected to the power grid using a classical single phase bridge rectifier working in the inverter mode of operation has been used. Unfortunately, such interconnection resulted in an excessive of reactive power generation from the grid and quite considerable distortion in the grid line current waveforms was noted. Also, in the main author's work [10], an alternate interconnection of the PVG with the grid was proposed. The interconnection used an H-Bridge controlled by a hysteresis controller. It was found that the proposed interconnection performance was limited by the fact that not all possible maximum power of the PVG source can be extracted. Extracting more power from the PVG source was at the expense of the deterioration and the distortion of the AC inverter current Waveforms.

In general, many of the research works related to grid-connected photovoltaic systems concluded that there are research gaps for unsolved issues that need to be considered with the intention of reaching better solar power quality production, and better power flow control of the grid-connected photovoltaic systems.

In this paper, a photovoltaic generator (PVG) is also tied to the power grid voltage supply through an AC/DC converter. The AC/DC converter is a power electronic converter able to work in a rectifier mode as well as in an inverter mode. What is also new in this contribution is that the buck-boost converter of Fig. 1 is replaced by a class D chopper [11]. The semiconductor switches of the class D chopper are gated by a high-frequency pulse whose duty cycle is controlled by the output of a perturb and observe (P&O) controller. This latter targets the operation of the PV generator near its maximum power points at any possible surrounding insolation and temperature levels. The other new and encouraging contribution in this paper is that the AC/DC converter is controlled by a voltage oriented controller (VOC). The principles of the voltage oriented controller are extracted from references [12-14]. The voltage oriented controller duties persist in conditioning the quality of the grid line currents waveforms and in preventing the grid voltage supply from generating or absorbing reactive power.

This paper is prepared in the following manner: Section 2 describes the study system by emphasizing mainly on the intended duties of main controller blocks, and section 3 presents the system simulations performance. References list related to the paper contribution is provided at the end of this article.

2. Study System Description

Fig. 2 illustrates the scheme of the proposed study system. Fig. 2(a) indicates the main blocks and shows the desired active/real power flows. Fig. 2(b) shows the six main components of the system which are (1) A three phase AC voltage source representing the phase 50-Hz power-grid, (2) a three phase feeder, (3) a three phase AC/DC bridge power electronic converter, (4) a shunt excited DC Motor connected to a point that is often known as the point of common coupling (PCC), (5) a class D chopper configuration, and (6) a DC voltage source representing the PVG array in series with a smoothing reactor.

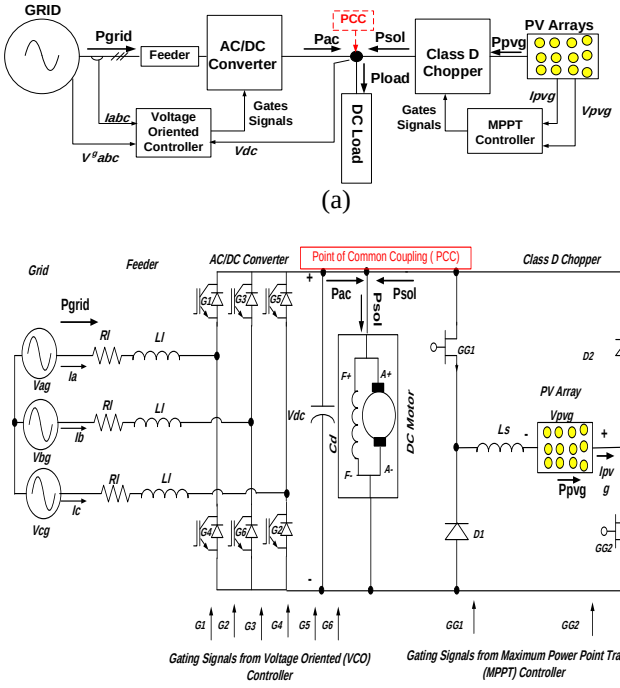

Fig2. Study System a) One Line Diagram b) Detailed Circuit

The next subsections describe the PVG characteristics and operation and function of the controllers shown in Fig. 2.

2.1 Photovoltaic Generator (PVG) Array

The photovoltaic generator (PVG) is made from a number of solar cells appropriately connected in series and parallel to generate DC electric power. The PVG array model does not differ in origin from the solar cell model. Details explanation about this latter is addressed in a number of relevant physics or microelectronics textbooks [15]. In this study, the PVG array consists of two basic series PV modules. The PVG module model is taken from Reference [16]. The name or type of PV array along with its I-V and P-V characteristics, under 1000W/m2 insolation and for two different temperatures 250C and 450C, are reproduced in Fig. 3.

As can be seen, the maximum power that can be delivered by the two series PV modules is 423.3 W

under 1000 W/m2 insolation level and 250C (i.e Standard conditions)

2.2 Maximum Power Point Tracker (MPPT) Controller

As shown in Fig. 2 (b), gating the semi-conductors (GG1 and GG2) of class D chopper can be provided by periodic pulses (GG1 and GG2). Each pulse should be characterized by a high frequency and a variable duty cycle. In fact, GG2 pulse is no more than GG1 pulse delayed by half period. Figure 4(a) depicts the controller block diagram that has been used to generate the gating signals GG1 and GG2 to class D chopper. It is worth to note that Class D chopper is operated in quadrant IV known usually as the regeneration mode quadrant. The duty cycle in such quadrant for each gating pulse (GG1 and GG2) should not exceed 50%.

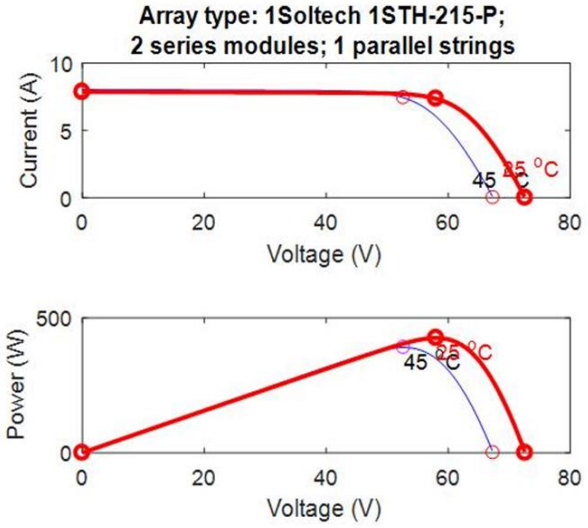

Fig 3. Photovoltaic Generator (PVG) Characteristics

a) I-V characteristics, b) P-V Characteristics

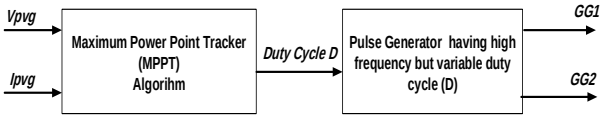

Fig4. Class D Chopper Gates Controller

Indeed, the value of the duty cycle D in this investigation is continuously decided by the output of a maximum power point tracker (MPPT) algorithm. Such algorithm performs its task according to the flowchart shown in Fig. 5. Such flowchart constitutes the content of the first block of Fig. 4 (i.e left block of Fig. 4). The MPPT algorithm performs its duty based on the idea of the Perturb and Observe (P&O) control technique [17]. The reason for using such a control technique is due to its robustness and its quick dynamic response. Moreover, such technique does not need to know neither the PV array surrounding insolation and temperature levels nor the surface state of the PV modules. Its task is to keep updating the operation of the PV array near its peak power values in which dP/dV=0. Where, P is the power delivered by the PV module and V is the voltage across its terminals.

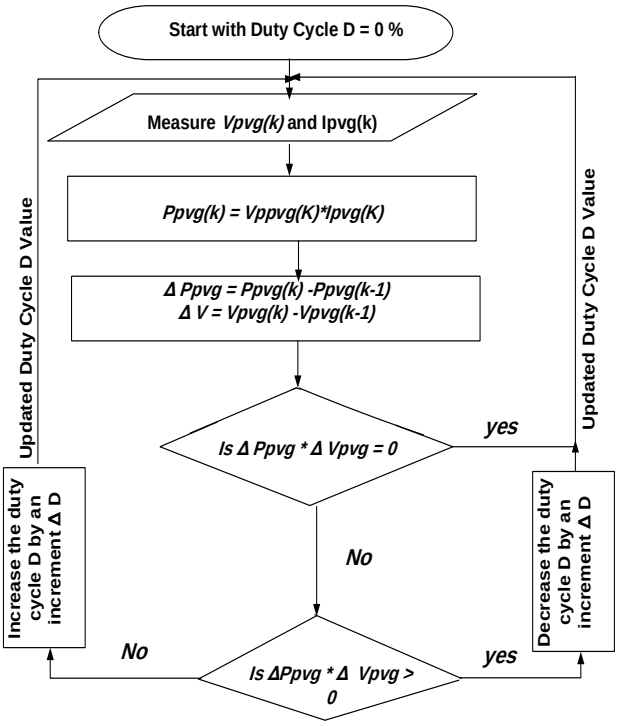

Fig 5. Maximum Power Point Tracker (MPPT) Algorithm

2.3 Voltage Oriented Controller (VOC)

The main objective of the voltage oriented controller (VOC) is to generate desired voltages $V^c_{a,b,c}$ ($V^c_{a,b,c}=[V^*_a \; V^*_b \; V^*_c]^T$) through proper switching states with a certain required phase shift from the grid phase voltages $V^g_{a,b,c}$ ($V^g_{a,b,c}=[V_{ag} \; V_{bg} \; V_{cg}]^T$) and by keeping the PCC bus dc- voltage shown in Fig. 2 at a certain desired or reference value [12-14].

Actually, the essence of the voltage oriented control (VOC) technique is to decompose the ac line current into two separate current components responsible of controlling the active and reactive powers flows. Indeed, the line current is split into a q-current component termed i_q and a d-current component termed i_d. Current i_d governs the active power flow while current i_q governs the reactive power flow. A unity power factor condition is obtained if the grid line currents $i_{a,b,c}$ are aligned with the grid phases voltages $V^g_{a,b,c}$. This condition occurs when a desired q-current component is set or fixed to zero ($i^*_q = 0$) [18].

Figure 6 represents the blocks diagram of the voltage oriented controller (VCO) that has been used in this investigation. It consists mainly of five blocks: Phase locked loop, abc-dq transformation, decoupled controller, dq-abc transformation, and PWM blocks. The Phase locked loop serves at finding an angle θ corresponding to the angle between a synchronous rotating d-axis frame and a fixed α-axis frame. The angle θ is used for all abc-dq and dq-abc transformation blocks.

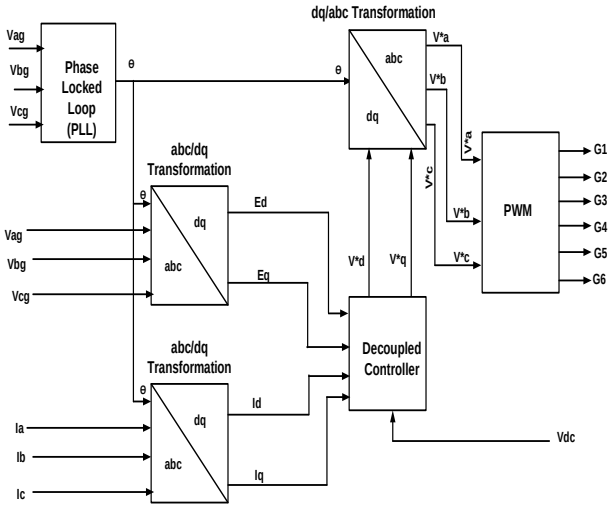

Fig 6. Voltage Oriented Controller (VCO) Block

The angle θ is continuously calculated as follows:

$$\begin{pmatrix} U\alpha \\ U\beta \end{pmatrix} = \sqrt{\frac{2}{3}} \begin{pmatrix} 1 & 1/2 & 1/2 \\ 0 & \sqrt{3}/2 & -\sqrt{3}/2 \end{pmatrix} \begin{pmatrix} \text{Vag} \\ Vbg \\ Vcg \end{pmatrix} \quad (1)$$

$$\theta = \arctan\left(\frac{U\beta}{U\alpha}\right) \quad (2)$$

The abc-dq transformation blocks perform their task by executing the following algebraic equations:

$$\begin{pmatrix} \text{Ed} \\ Eq \end{pmatrix} = A(\theta) \begin{pmatrix} \text{Vag} \\ Vbg \\ Vcg \end{pmatrix} \quad and \quad \begin{pmatrix} \text{id} \\ iq \end{pmatrix} = A(\theta) \begin{pmatrix} \text{ia} \\ ib \\ ic \end{pmatrix} \quad (3)$$

Where

$$A(\theta) = \sqrt{\frac{2}{3}} \begin{pmatrix} \cos(\theta) & \cos(\theta + \frac{2\pi}{3}) & \cos(\theta - \frac{2\pi}{3}) \\ \sin(\theta) & \sin(\theta + \frac{2\pi}{3}) & \sin(\theta - \frac{2\pi}{3}) \end{pmatrix}$$

Note Vag, Vbg, Vcg are the grid phase voltages whereas ia, ib, ic are the grid line currents. The content of the decoupled block is shown in Fig. 7.

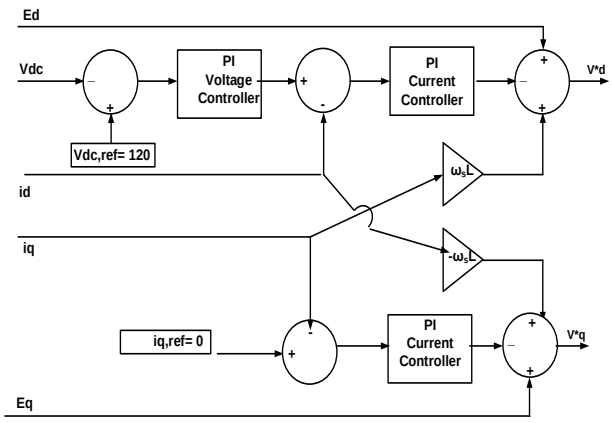

Fig 7. Contents of the Decoupled Controller of Fig. 6

The decoupled controller block contains three Proportional-Integrator (PI) controllers: Two PI current controllers and one PI voltage controller. The intention behind the operation of a proper decoupled controller is to have the measured PCC point DC voltage bus near a pre-set or a reference DC voltage (Vdc,ref). Moreover, the decoupled controller has the duty of forcing the q-component current (iq) of the line currents to be zero (iq,ref=0) when reaching steady state conditions. In doing so the reactive power delivered or absorbed by the grid becomes null. This will correspond to a unity power factor at the power grid bus.

The transformation of the voltage components V_d^* and V_q^*, obtained as outputs of the decoupled controller, to the controlled phase voltages V_a^*, V_b^*, and V_c^* is done through the dq-abc transformation block. This is done mathematically as :

$$\begin{pmatrix} V_a^* \\ V_b^* \\ V_c^* \end{pmatrix} = \begin{pmatrix} \cos(\theta) & \sin(\theta) \\ \cos(\theta - \frac{2\pi}{3}) & \sin(\theta - \frac{2\pi}{3}) \\ \cos(\theta + \frac{2\pi}{3}) & \sin(\theta + \frac{2\pi}{3}) \end{pmatrix} \begin{pmatrix} V_d^* \\ V_q^* \end{pmatrix} \quad (4)$$

The last three controlled voltages V_a^*, V_b^*, V_c^* are fed as inputs to a pulse width modulation block (PWM block of Fig. 6). The PWM is responsible of generating convenient pulses to the gates of the IGBTs switches of Fig. 2(b). The gate pulses are generated by going through the tabulation of the logic operations or steps shown in Fig. 8.

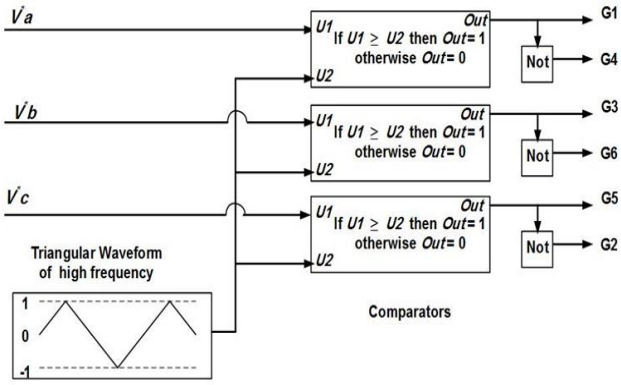

Fig 8. Pulse Width Modulation (PWM) Block Content

3. Study System Performance

The performance of the proposed energy system of Fig. 2 has been investigated and evaluated via extensive simulation studies done in MATLAB Simulink platform. The SIMULINK files of the developed models for the studied system can be obtained by contacting the main author of this paper. The used system data are shown in Table 1.

Table 1. Study System Data

Three Phase Power Grid Voltage			
RMS line to line Voltage: $24\sqrt{3}$ V		Frequency: 50 Hz	
Feeder			
Series Resistance: Rf =7 mΩ		Series Inductance Lf= 1 mH	
Photovoltaic Generator Module Type 1 Soltech – 1STH-215p Maximum Power ***Pm*** 213.15 W			
Open Circuit Voltage ***Voc*** : 36.3 V		Voltage at maximum power point ***Vm*** : 29 V	
Short-circuit current ***Isc*** : 7.84 A		Current at maximum power point ***Im*** : 7.35 A	
Series smoothing Inductance Ls= 50 mH			
PCC Smoothing DC Capacitor **Cd =** 1000 µF			
Voltage Oriented Controller (VCO) Reference Values			
Vdc,ref = 120 V		**Iq, Ref** = 0 A	
VCO Decoupled Controller PI Blocks Parameters			
PI voltage controller constants		PI Current controller constants	
Kp = 0.01	**Ki** = 10	**Kp** = 5000	**Ki** = 20000
Class D Chopper			
Gates Pulses Frequency1000 Hz		Gates Pulses Duty cycle Limited between 0 to 50 %	
Shunt Excited DC Motor Load			
Armature winding	Resistance **Ra=** 5.15 Ω	Inductance **La=** 12 mH	
Field winding	Resistance **Rf=** 120 Ω	Inductance **Lf** = 600 mH	
Armature Constant **Kaϕ=** 1.0 V.s	Inertia Constant **J** = 0.1 kg.m2	Applied Load Torque **Tl=** 1.25 Nm	

Assuming certain daily insolation patterns, the performance of the proposed hybrid energy system is assessed based on recording the following measurements:

- Active power contributions by the PV and grid systems to the DC load
- The voltage level at the PCC DC bus and its comparison with a desired reference bus voltage (Vdc,ref).
- Power Factor value at the power grid bus
- The level of q-current component iq and compared with its reference value. (iq,ref).
- Total Harmonic distortion factor (THD) level in the grid line currents
- RMS value of the grid line current.
- The level of the duty cycle of the pulses supplied to the gate of class D chopper controlled switches.

Figure 9 depicts the daily (from 6:30 am to 6 pm) pattern of the active or real powers at the point of common coupling (PCC). As can be seen clearly from Fig. 9(b) the DC load gets its constant power regardless of the change that may occur in the insolation level (Fig. 9 (a)). Examining Fig. 9(c), one can deduce the PV system has injected its real/active power to the PCC point and its amount depends on the surrounding insolation level. The injected solar power is always near its possible maximum power point (MPP). This demonstrates that the maximum power point tracker (MPPT) controller has adequately performed its intended task. Figure 9(d) indicates the active or real power drawn from or supplied to the power grid source. Actually, the results depicted in Fig. 9(d) indicate that the AC/DC converter played two roles/modes: the role of rectifier when the active power is drawn from the grid and the role of inverter when the active power is supplied to the grid.

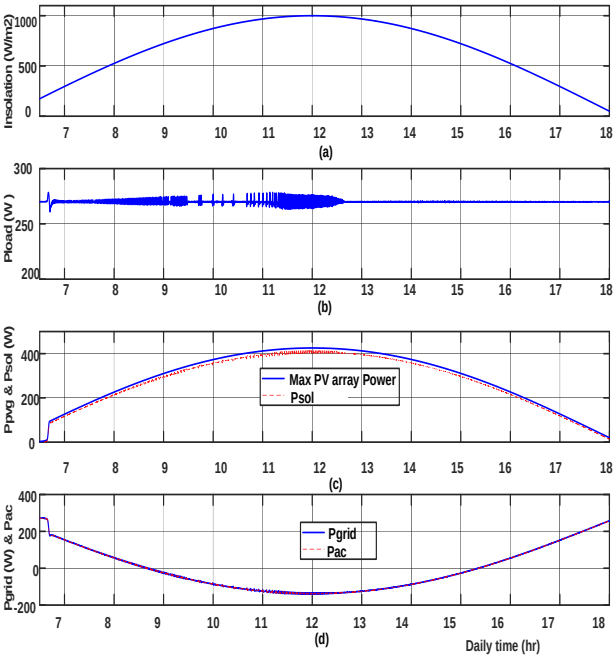

Fig 9. Active Powers Flow

a) Pretended Daily Insolation Level b) DC load Power c) PV Array Power Contribution d) Grid Power Contribution

Figure 10 indicates the performance of the voltage oriented controller (VOC). Figure 10(b) represents the online computed power factor at the grid voltage bus. It is clearly shown that when the AC/DC converter plays the role of rectifier the power factor is unity. This is equivalent of saying the grid does not supply any amount of reactive power. Similarly, when the AC/DC converter plays the role of the inverter, the power factor is also unity (-1 is shown in Fig. 10(b) to indicate inverter mode) and this is equivalent of saying that the grid neither does not absorb any amount of reactive power.

Figure 10(c) represents the total harmonic distortion (THD) levels in the grid line currents. The obtained THD levels are ought to be checked whether they fall-in or not fall-in within the allowable standard limits [19-20]. One interesting remark to note is that near the transition from rectifier mode to inverter mode and vice versa (from inverter mode to rectifier mode), the recorded THD levels are quite high. Worries about such remark should be eased because the overall rms value of the whole grid line current is near zero at such transitions, as shown in Fig. 10 (d). This is to say the distortion in the line currents will have very minor effects on the overall system performance such transitions because all fast Fourier transform (FFT) components of the line currents, including the fundamental component, will be of small magnitudes.

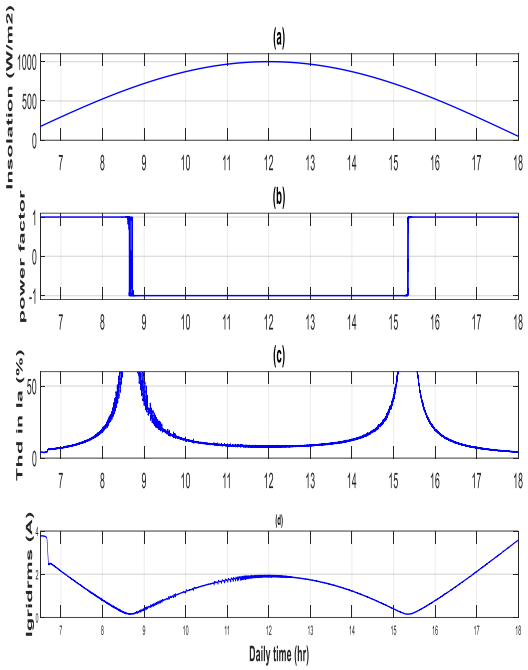

Fig 10. Voltage Oriented Controller (VCO) Performance a) Pretended Daily Insolation Level b) Power Factor at Grid Voltage bus c) Total Harmonic Distortion (THD) level in Grid Lines Currents d) Rms Value of the Grid Line Currents

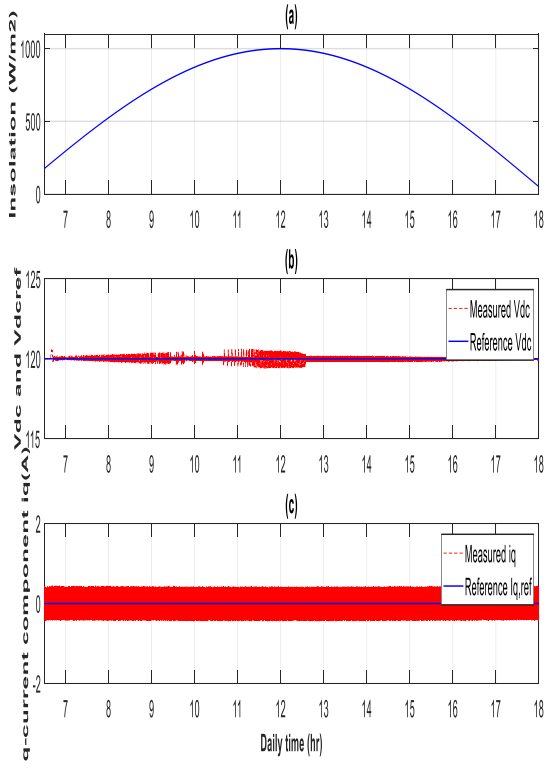

Fig 11. Voltage Oriented Controller Performance a) Pretended Daily Insolation Level b) DC Voltage at the PCC bus c) q-current component (iq) level

Figure 11 represents also the performance of the voltage oriented controller (VOC). Figure 11(b) depicts the online measurement of the PCC DC voltage and its compared to its desired reference voltage (Vref=120 V). A quite good compatibility is noted between the two voltages. Figure 11 (c) depicts the level of the q- current component of the line current (iq). As it is seen, it sticks oscillating near its zero reference value (iq,ref=0 A). The obtained levels of the q-current component confirm that the reactive power is neither absorbed nor delivered by the power grid. This has been already manifested by recording a unity power factor level at the power grid bus, as shown previously in Fig. 10 (b).

As to the performance of the maximum power point tracker (MPPT), Fig. 12 (b) shows clearly that the power extracted from the PV array is always near the maximum PV modules power. Figure 12(c) depicts the online duty cycle values of the pulses supplied to gates of class D chopper controlled semiconductors. Such duty cycles values are noted to be below 50 % level and this is to confirm that class D chopper is always operated in quadrant IV (i.e regeneration mode).

Figure 13 depicts one steady state cycle of the time domain waveforms of the grid voltages and the grid line currents under minimum and maximum insolation levels, under 50 W/m2 and 1000 W/m2 respectively. It is clearly seen that under minimum insolation level, the grid phase voltages and grid line currents are in phase. Thus, the AC/DC converter is operated in a rectifier mode and the power factor is equal to one. Similarly, under maximum insolation level, the grid phase voltages and grid line currents are out of phase. Hence , the AC/DC converter is worked in an inverter mode and the power factor is also equal to one (i.e unity).

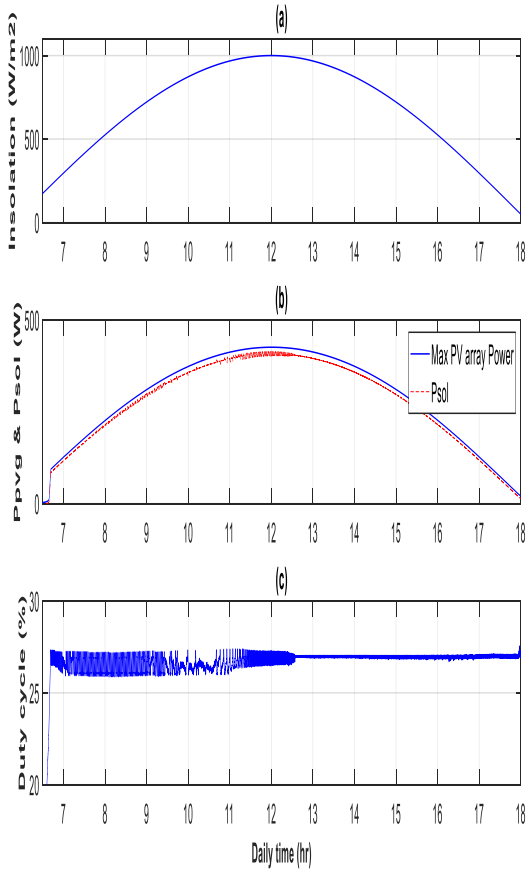

Fig 12. Maximum Power Point Tracker Controller Performance a) Pretended In Daily solation Level b) PV array Power c) Duty Cycle Level of the MPPT controller

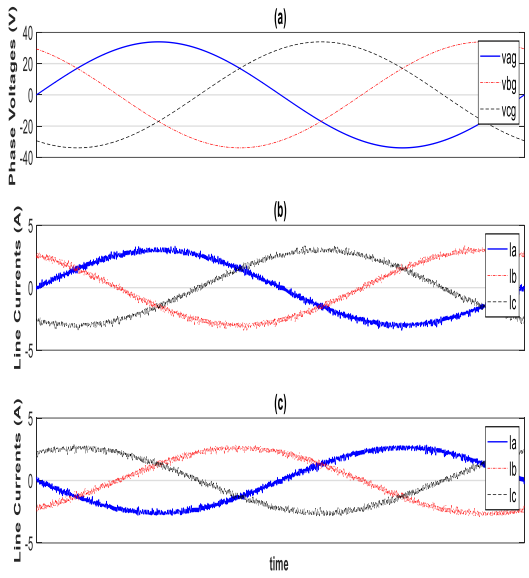

Fig 13. Grid Phase Voltages and Grid Line Currents a) Phase Voltages b) Line Currents under Minimum Insolation Level c) Line Currents under Maximum Insolation Level

4. Conclusion

An interconnection of a hybrid energy system consisting of a PV system and a three phase AC power grid feeding a shunt DC motor with a constant load power through an AC/DC converter has been investigated. The proposed interconnection contains a class D chopper besides an AC/DC converter.

The class D chopper performed the job of a maximum power point tracker (MPPT) adequately. The Class D chopper was controlled by the perturb and observe (P&O) control technique.

The AC/DC converter was controlled by a voltage oriented (VOC) controller. The AC/DC converter was able to operate in rectifier mode as well as in inverter mode. The voltage oriented controller (VOC) prevented the AC grid from drawing or generating reactive power. Moreover, the voltage oriented controller (VOC) conditioned the quality of the grid line currents to a certain acceptable extent. Extensive Simulink simulations results had demonstrated and validated the satisfactory performance of the proposed hybrid energy interconnection.

Future work is to confirm or enhance the performance of the proposed interconnection by the practical implementation of the proposed interconnection.

References

[1] K. N. Nwaigwe, P. Mutabilwa, and E. Dintwa, "An overview of solar power (PV systems) integration into electricity grids", Materials Science for Energy Technologies (2019), Vol 2, pp. 629–633.

[2] S. E. Binti Sabri, M. Z. Bin Sujod, W. N. H. Binti Alias, and M. S. Bin Jadin, "Limiting THD of Grid Connected Photovoltaic System using PWM Switching Frequency Selection Based on Solar Irradiance Changing", 2019 IEEE International Conference on Automatic Control and Intelligent Systems (I2CACIS), DOI: 10.1109/I2CACIS.2019.8825091, Selangor, Malaysia, 29th June 2019.

[3] L. Hassaine, and M. R. Bengourina, "Control technique for single phase inverter photovoltaic system connected to the grid", Energy Reports (2020), pp. 200-209.

[4] X. Weidong, E. Ammar, K. Vinod, and H. Z. Hatem, "Overview of maximum power point tracking technologies for photovoltaic power systems", IECON 2011 - 37th Annual Conference on IEEE Industrial Electronics Society, Melbourne, (7-10 November 2011), pp. 3900 – 3905.

[5] W. Teulings, J. C. Marpinard, A. Capel, and D. O'Sullivan, " A new maximum power point tracking system", IEEE Annual Power Electronics Specialists Conference (PESC'93), DOI: 10.1109/PESC.1993.472018, Washington Seattle, (20-24 June 1993).

[6] A. S. Alexander, " Development of solar photovoltaic inverter with reduced harmonic distortions suitable for Indian sub-continent", Renewable and Sustainable Energy Reviews (2016), Vol. 56, pp. 694-704.

[7] A. Hassan, A. M. Azmy., D. M. Yehia, Z. and Gurgi, "Harmonic Reduction for Grid-Connected Photovoltaic System based on Multilevel Inverter", Australian Journal of Basic and Applied Sciences (2018), DOI: 10.22587/ajbas.2018.12.9.23, Vol. 12, pp. 135-145.

[8] T. Oukhoya, A. H. Sandali, and A. Cheriti, " Improved Grid-Connected PV System based on SVPWM Inverter and using P-V Optimal Slope MPPT Technique", International Journal of Applied Information Systems (IJAIS) (2015), Vol. 10, pp. 18-24.

[9] M. Taleb, "Interconnection of a Photovoltaic Generator (PVG) to the Main Supply: A Simulation Study", Renewable Energy and Power Quality Journal (2011) , Vol. 9, Paper 396.

[10] M. Taleb, N. Mansour., and K. Zehar , " An Improved Grid Tied Photovoltaic System Based on Current Conditioning", JESTECH Journal of Engineering Sciences and Technology: An International Journal (2018), Vol. 21, pp.1113-1119.

[11] M. D. Singh, and K. B. Khanchandani, Power Electronics, 2nd Edition, Mc Graw Hill Companies, 2008.

[12] M. Malinowski, M. P. Kazmierkowski. and A. M. Trzynadlowski, "A comparative study of control techniques for PWM rectifiers in AC adjustable speed drives" IEEE Trans. on Power Electronics (2003), Vol. 18, pp. 1390-1396.

[13] M. P. Kazmierkowski, F. Blaabjerg, and R. Krishnan, " Control in power electronics, selected problem", Elsevier Science, USA., 518p, (2002). ISBN : 0-12-402772-5.

[14] M. P. Kazmierkowski, "Current Control Techniques for Three-Phase Voltage-Source PWM Converters: A Survey", IEEE Transactions on Industrial Electronics (1998), Vol. 45, pp. 691–703.

[15] A. S. Sedra, and K. C. Smith, Microelectronic Circuits, Oxford University Press (2006), London, UK.

[16] P. Gilman, and A. Dabos, , System Advisor Model SAM 2011.12.2: General Description, Renewable Energy Laboratory (NREL), Technical Report NREL/TP-6A20-534372012.

[17] M. A. Elgendy, B. Zahawi, and D. J. Atkinson, "Evaluation of perturb and observe MPPT algorithm implementation techniques", 6th IET International Conference on Power Electronics, Machines, and Drives (PEMD) (2012), DOI: 10.1049/cp.2012.0156, Bristol, 27-29.

[18] R. Guzman, L. G. De Vicuña, M. Morales, M. Castilla and J. Matas, "Sliding-Mode Control for a Three-Phase Unity Power Factor Rectifier Operating J. Fixed Switching Frequency", IEEE Trans. Power Electronics (2016), Vol. 31, No,1, pp. 758-769.

[19] IEEE Power and Energy Society (2014). IEEE Recommended Practice and Requirements for Harmonic Control in Electric Power Systems IEEE Std 519™-, IEEE Standards Association, (2014).

[20] S. M. Halpin., "Comparison of IEEE and IEC harmonic standards", Power Engineering Society General Meeting, DOI: 10.1109/PES.2005.1489688, (2005).